Current Medical Science
DOI https://doi.org/10.1007/s11596-018-1848-7
38(1):70-77,2018

Bioinformatics Analysis of Genes and Pathways of CD11b^{+}/Ly6C^{intermediate} Macrophages after Renal Ischemia-Reperfusion Injury*

Dong SUN (孙 冬)[1†], Xin WAN (万 辛)[1†], Bin-bin PAN (潘斌斌)[1], Qing SUN (孙 晴)[2], Xiao-bing JI (嵇小兵)[1], Feng ZHANG (张 峰)[1], Hao ZHANG (张 浩)[1], Chang-chun CAO (曹长春)[1,2#]

[1]*Department of Nephrology, Nanjing First Hospital, Nanjing Medical University, Nanjing 210006, China*
[2]*Department of Nephrology, The Affiliated Sir Run Run Hospital, Nanjing Medical University, Nanjing 211166, China*

Summary: Renal ischemia-reperfusion injury (IRI) is a major cause of acute kidney injury (AKI), which could induce the poor prognosis. The purpose of this study was to characterize the molecular mechanism of the functional changes of CD11b^{+}/Ly6C^{intermediate} macrophages after renal IRI. The gene expression profiles of CD11b^{+}/Ly6C^{intermediate} macrophages of the sham surgery mice, and the mice 4 h, 24 h and 9 days after renal IRI were downloaded from the Gene Expression Omnibus database. Analysis of mRNA expression profiles was conducted to identify differentially expressed genes (DEGs), biological processes and pathways by the series test of cluster. Protein-protein interaction network was constructed and analysed to discover the key genes. A total of 6738 DEGs were identified and assigned to 20 model profiles. DEGs in profile 13 were one of the predominant expression profiles, which are involved in immune cell chemotaxis and proliferation. Signet analysis showed that Atp5a1, Atp5o, Cox4i, Cdc42, Rac2 and Nhp2 were the key genes involved in oxidation-reduction, apoptosis, migration, M1-M2 differentiation, and proliferation of macrophages. RPS18 may be an appreciate reference gene as it was stable in macrophages. The identified DEGs and their enriched pathways investigate factors that may participate in the functional changes of CD11b^{+}/Ly6C^{intermediate} macrophages after renal IRI. Moreover, the vital gene Nhp2 may involve the polarization of macrophages, which may be a new target to affect the process of AKI.
Key words: renal ischemia-reperfusion injury; macrophage; differentially expressed genes; series test of cluster; functional enrichment analysis; protein-protein interaction

Acute kidney injury (AKI) is a significant health problem that is characterized by rapid kidney function decline, and an incidence of roughly 14 per 1000 admissions[1–3]. The mortality could rise to 11% one week after the occurrence of AKI, and to 38.1% at five years in severe AKI patients[4, 5]. Renal ischemia-reperfusion injury (IRI), including hypotension or shock in developed countries and dehydration in other countries, is a major cause of AKI[5].

IRI can result in tubular vacuolization, edema, infarction, cast formation, and neutrophil infiltration[6]. Some immune cells can affect the progression of AKI[7–9]. For example, macrophages could cause renal injury, facilitate renal repair, and cause fibrosis after IRI. Within 24 h after IRI, monocytes are recruited to the kidney and differentiate into macrophages[10]. M1 macrophages accumulate soon after IRI, promoting a proinflammatory milieu and worsening the level of tu-

Dong SUN, E-mail: sundong@njmu.edu.cn; Xin WAN, E-mail: wanxin@njmu.edu.cn
†The authors contributed equally to this work.
#Corresponding author, E-mail: caochangchun@njmu.edu.cn
*This work was supported by grants from the National Natural Science Foundation of China (No. 81670634), Graduate student scientific research innovation projects in Jiangsu province (No. KYLX15_0981), and Nanjing Medical University Science and Technology Development Fund (No. 2016NJMU065).

bule injury. A subsequent switch to M2 macrophages can suppress the inflammatory response and induce a proliferative repair phase[11]. M2 macrophages are involved in producing extracellular matrix components, but may also contribute to the tissue fibrosis, should this process become dysregulated[12].

The marker of macrophages may be diverse in different organs, therefore defining macrophages according to their function has become challenging[13]. According to the whole genome microarray analysis data, the $CD11b^+/Ly6C^{high}$ population was associated with the onset of renal injury and produced proinflammatory cytokines. In addition, the $CD11b^+/Ly6C^{int}$ population demonstrated a wound healing phenotype[14]. Dragomir *et al* reported that $CD11b^+/Ly6C^{lo}$ cells were larger than $CD11b^+/Ly6C^{hi}$ cells, and more irregularly shaped. Moreover, $CD11b^+/Ly6C^{lo}$ cells contained a highly vacuolated cytoplasm and an increased cytoplasm:nuclear ratio. RT-PCR analysis revealed that mRNA expression levels related to proinflammatory proteins (for example, TNF-α, iNOS, and the chemokine receptor CCR2) were significantly higher in $CD11b^+/Ly6C^{hi}$ cells than in $CD11b^+/Ly6C^{lo}$ cells. In contrast, the mRNA expression level of anti-inflammatory cytokine IL-10 was reduced in $CD11b^+/Ly6C^{hi}$ cells when compared to $CD11b^+/Ly6C^{lo}$ cells[15]. Clements *et al* investigated the genes that were uniquely expressed in each population. It is necessary to consider of genes that were regulated in each phenotype over time[14].

The purpose of our study was to evaluate the proportion of macrophages that changed at different time points after IRI. We used microarray analysis to identify the differentially expressed genes (DEGs) in $CD11b^+/Ly6C^{int}$ macrophages of C57BL/6 mice and mice undergoing sham surgery or IRI for 4 h, 24 h or 9 days. We used The Series Test of Cluster (STC) analysis, STC-Gene Ontology analysis and pathway analysis to identify changes in function and pathways in macrophages in the different groups. The protein-to-protein interaction (PPI) network was applied to select key genes by degree, which may help explain how macrophages were influenced at different time points. Our study may provide further insight into a new target that affects the process of AKI by changing the macrophage function.

1 MATERIALS AND METHODS

1.1 Data Pre-processing

Gene expression analysis was performed on an Affymetrix Mouse Genome 430 2.0 Array platform (Affymetrix, USA) for which the transcription profile GSE75808 from the Gene Expression Omnibus (GEO) database, an open-access functional genomics data repository was downloaded. Twenty-five male C57BL/6 mice (8 to 10 week-old) were divided into several groups and underwent either bilateral renal IRI for 28 min or sham surgery followed by reperfusion. For RNA isolation and amplification for cDNA production, macrophage populations were sorted on a BD FACSARIA II cell sorter (BD Bioscience,usA) based on $CD11b^+/Ly6C^{high}$, $CD11b^+/Ly6C^{int}$ or $CD11b^+/Ly6C^{low}$ as previously described[14]. We analysed the expression of $CD11b^+/Ly6C^{int}$ macrophages of the sham (GSM1968232 and GSM1968235), 4-h IRI (GSM1968226, GSM1968228 and GSM1968230), 24 h IRI (GSM1968216, GSM1968217 and GSM1968218) and 9 day IRI (GSM1968219, GSM1968221 and GSM1968223) groups to identify genes that are associated with this subset of macrophages.

1.2 DEGs Analysis

The probe-level data were converted into expression measures so that by taking the average expression value, the expression values of all probes for a given gene in each sample were reduced to a single value[16]. Next, the principal component analysis (PCA) was performed and DEGs were identified as previously described[17]. In our study, we used the effective statistical method for small samples to identify differentially expressed mRNAs among the four groups of macrophages by GCBI (https://www.gcbi.com.cn/gclib/html/index). These values include false discovery rate-adjusted *P* values and were considered significant when $P<0.05$.

1.3 STC Analysis

To validate the most probable set of clusters of four-time series, we used the STC algorithm of gene expression dynamics to profile the gene expression time series as previously described[18]. The STC algorithm identified which profiles have a significant number of genes assigned and the result may indicate the change rule of samples at different time points.

1.4 STC-Gene Ontology Analysis

To identify functional changes in macrophages, we analysed the role of DEGs in each significant expression profile. Analyses were based on the Gene Ontology (GO) database in Funrich 3.0 software as previously described[19]. The DEGs of each significant expression profile was classified into a group of biological process categories from GO annotation. GO terms were considered significant at $P<0.05$.

1.5 Pathway Analysis

We identified the significant pathways that were changed in $CD11b^+/Ly6C^{int}$ macrophages. To identify the main biological function of $CD11b^+/Ly6C^{int}$ macrophages, pathways of genes with similar expression trend were analysed. Analyses were based on the Reactome database in Funrich. The threshold of significance was considered as $P<0.05$.

1.6 PPI Network Construction Analysis

We created a PPI network to analyse the key genes

which regulate other genes. Based on the 927 DEGs in profile 13, PPI was analysed by STRING 10.5 and the cytoHubba app of Cytoscape software (version 3.5.1) as previously described[20]. The combined score of the PPI value was>0.4. Genes that showed a high degree were identified as key genes as previously described[21].

CytoHubba is an approach that has frequently been used to select hub genes, and provides 11 topological analysis methods, including Degree, Maximum Neighborhood Component, Edge Percolated Component, Maximal Clique Centrality, Density of Maximum Neighborhood Component, and six centralities (Bottleneck, EcCentricity, Closeness, Betweenness, Radiality, and Stress) based on the shortest paths[22]. Genes that appeared in the top 50 genes by more than 6 ways in CytoHubba were identified. The top 50 hub forming genes were output by each of the ranking methods as a measure of significance. Genes were considered significant when they were identified by both methods. We especially focused on the genes of the top 20 degrees in the PPI network as previously described[23].

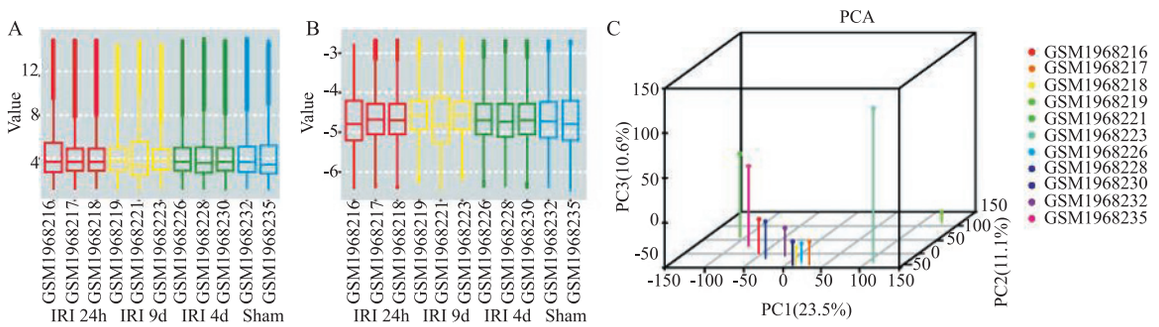

Fig. 1 Data processing before filtering differentially expressed genes (DEGs)
A and B: box-plot of expressed data before and after normalization. Vertical axis represents expression values and horizontal axis represents the sample name. The line in the box represents the data median in each group, whose distribution represents the degree of standardization of data; C: principal component analysis (PCA) scores plot of four groups

2 RESULTS

2.1 Identification of DEGs

In this study, we analysed DEGs from CD11b^{+}/Ly6C^{int} macrophages, which were isolated from kidneys of mice undergoing sham surgery (n=2), and IRI at 4 h, 24 h, and 9 days (n=3 per group). Figure 1A and 1B present the data before and after normalization. In fig. 1C, the PCA score plots of the four groups are shown. A total of 6738 normalized DEGs were identified (P<0.05 and q<0.05) at different time points.

2.2 Cluster Analysis

To identify target genes among the 6738 genes, twenty expression profiles were evaluated by cluster analysis. Each profile contained genes with a similar expression pattern after IRI. Among the 20 profiles of genes, nine profiles (profile 13, 5, 10, 2, 4, 7, 11, 1 and 3) were significantly different (P<0.05) (fig. 2 and table 1).

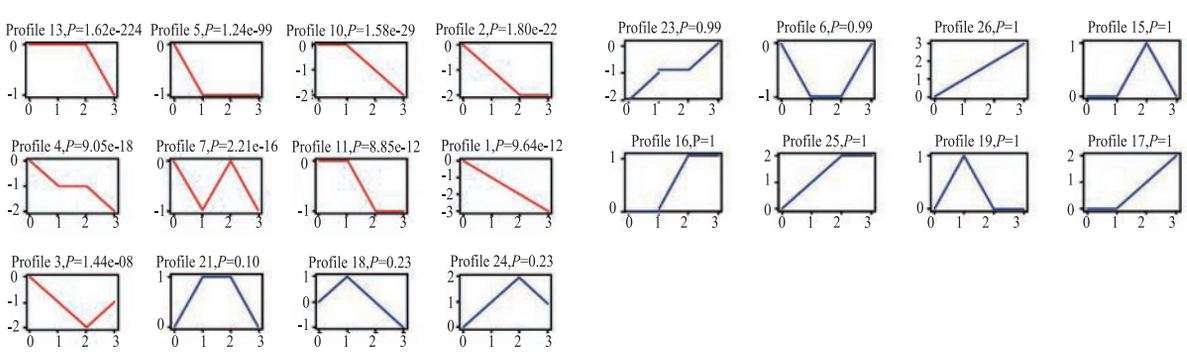

Fig. 2 Series test of cluster (STC) analysis for DEGs of CD11b^{+}/Ly6C^{int} macrophages derived from sham operated mice and from mice 4 h, and 1 and 9 days after renal ischemia-reperfusion injury (IRI)

Table 1 Differentially expressed genes grouped into expression profiles by cluster analysis

Profile number	Genes expected[#]	Genes assigned[*]	*P* value
Profile13 (0, 0, 0, -1)	1191	415.58	1.63E-224
Profile5 (0, -1, -1, -1)	1430	798.83	1.24E-99
Profile10 (0, 0, -1, -2)	262	120.33	1.58E-29
Profile2 (0, -1, -2, -2)	311	170.96	1.80E-22
Profile4 (0, -1, -1, -2)	271	154.67	9.05E-18
Profile7 (0, -1,0, -1)	721	529.29	2.21E-16
Profile11 (0,0, -1, -1)	451	324.71	8.85E-12
Profile1 (0, -1, -2, -3)	120	60.63	9.64E-12
Profile3 (0, -1, -2, -1)	277	195.17	1.44E-08

[#]: the expected number of genes that are randomly assigned to the model profile. [*]: the actual number of genes that are assigned to the model profile. *P* values indicate the significance levels between expected and actual numbers of genes.

2.3 STC-Gene Ontology Analysis

As shown in table 2, GO terms that were downregulated after renal IRI included cell cycle, inflammatory response, apoptosis, oxidation-reduction process, autophagy, and cell proliferation. Profile 13 consisted of genes that were stable at early time points and then rapidly decreased at later time points. To get insights into the biological effects of the genes in profile 13, we analysed the involved GO terms using the GO annotation in Funrich 3.0 (the threshold of GO terms was $P<0.05$). Biological processes such as transport and apoptosis showed the most notable enrichment of the target genes. Moreover, chemotaxis of several immune cells was also decreased at day 9 after IRI. Among the cellular component, extracellular vesicular exosome and mitochondrion showed a maximum enrichment, whereas protein binding and RNA binding showed the highest enrichment of molecular function (fig. 3).

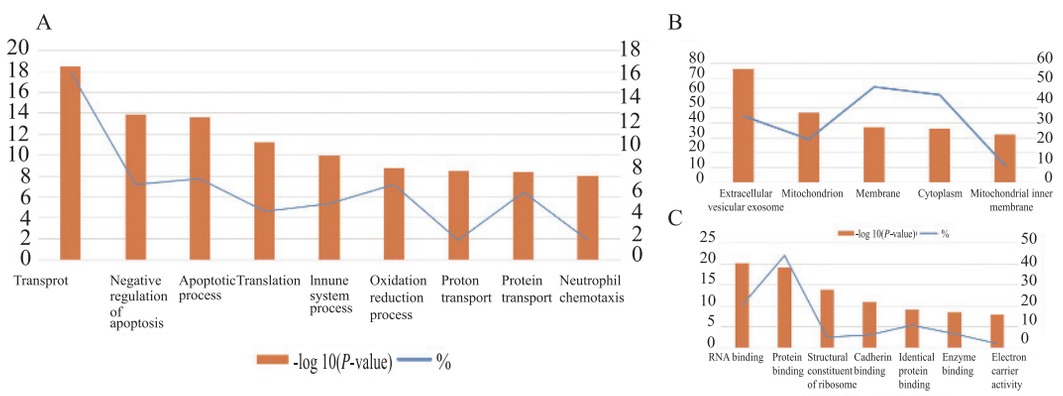

Fig. 3 Series test of cluster-Gene Ontology analysis of differentially expressed genes in profile 13
A: biological process; B: cellular component; C: molecular function

2.4 Pathway Analysis

We analysed the pathway enrichment using Reactome database for DEGs of profile 13. $P<0.05$ was considered for pathway analysis. The highest enrichment of pathway was demonstrated for neutrophil degranulation (P=1.01e-41) and respiratory electron transport (P=1.47e-17) (fig. 4).

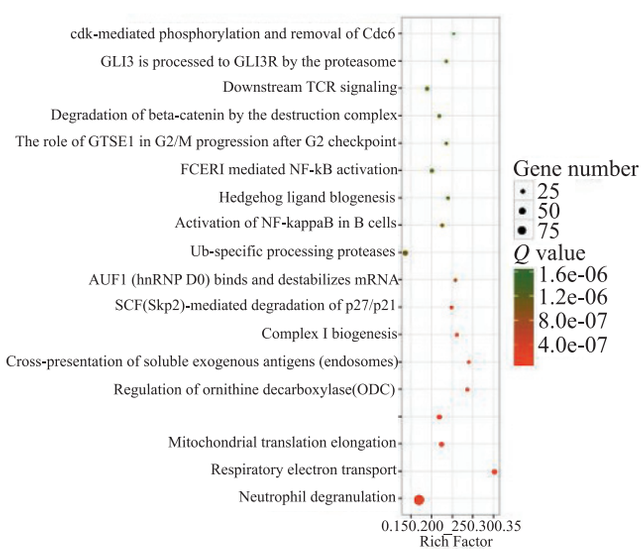

Fig. 4 Pathway enrichment analysis of differentially expressed genes in profile 13

2.5 Network Analysis

STRING analysis was used to obtain the PPI of the 927 DEGs in profile 13. The minimum required interaction score was 0.4. We gained a total of 6903 edges and 902 nodes, accounting for 97.30% of all DEGs. Results demonstrated that Gapdh (degree: 138), Hsp90aa1 (degree: 110), Actb (degree: 90), Actg1 (degree: 81), Atp5a1 (degree: 74), Atp5o (degree: 69), Cdc42 (degree: 68), Pcna (degree: 66), Uqcr11 (degree: 65) and Cox4i1 (degree: 60), which all have a high degree, were identified as hub genes in the PPI network (fig. 5). Moreover, Rhoa, Rac2, Nhp2, Rplp0, Rpl5, Rpl7, Ppp2ca, Mrpl2, and Rps6 were among the top twenty degrees in the PPI network.

Table 2 Brief introduction of fundamental functional categories in significantly different expression patterns

	Profile 13	Profile 5	Profile 10	Profile 2	Profile 4	Profile 11	Profile
Cell cycle, inflammatory response, apoptosis and oxidation-reduction process	√	√	√	√	√	√	√
Autophagy	√	√	√		√	√	√
Cell proliferation	√	√	√				
Cell death	√	√			√		
SnRNA pseudouridine synthesis	√		√				
G1/S transition of mitotic cell cycle	√			√			
Cell migration and monocyte chemotaxis	√						

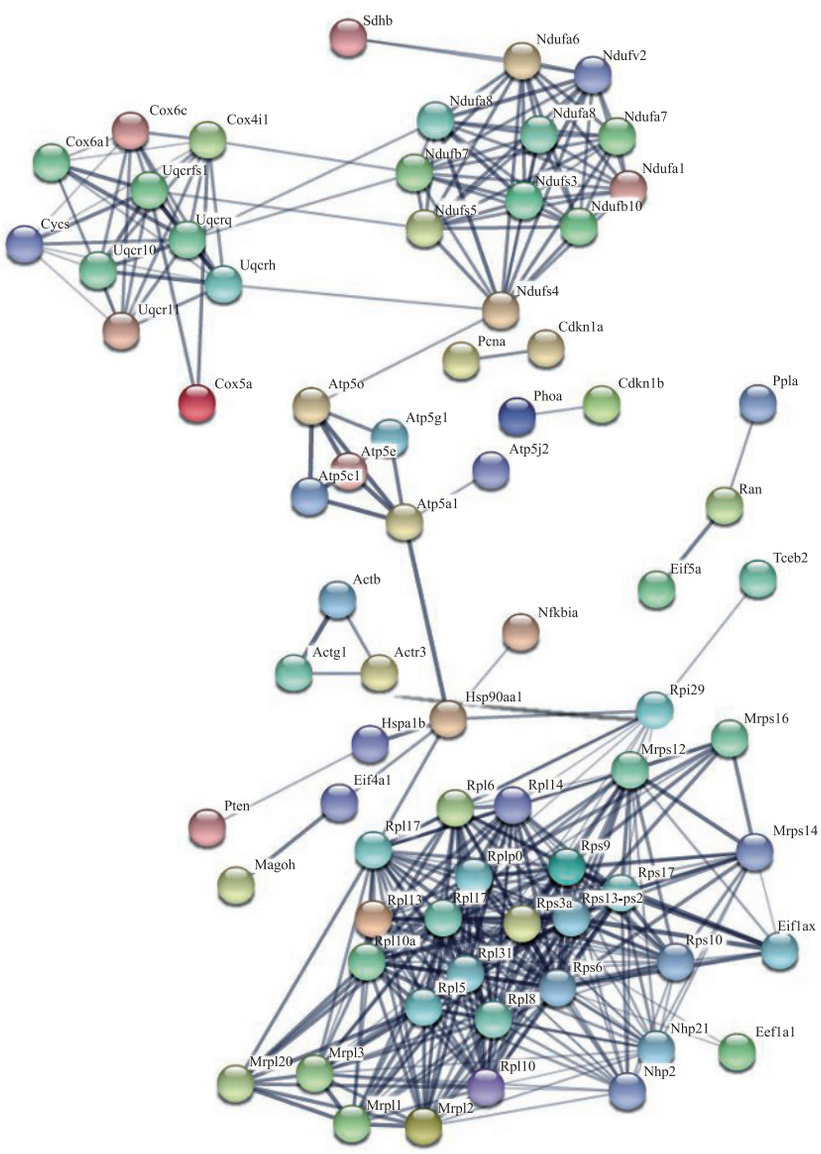

Fig. 5 Interaction network analysis of differentially expressed genes in profile 13

Cycle nodes represent genes. The edges between two nodes are thicker when the combined score is higher identified by experiments. We chose genes of the top 100 degrees to visualize the protein-to-protein interaction (PPI)

In addition to STRING analysis, key genes were also identified by CytoHubba. Table 3 presents genes that were considered to be the top 50 key genes in more than 6 ways of the 11 topological analysis methods described above. Because the changes of the genes with either a high degree or selected by Cytohubba could regulate the expression of multiple genes, they were identified as key genes for further study.

Table 3 Lists of genes representing the top 50 key genes in more than 6 ways

Genes	A total of ways for selecting the gene	Genes	A total of ways for selecting the gene	Genes	A total of ways for selecting the gene
Rpl10	10	Atp5o	8	Tlr2	7
Actb	9	Cd40	8	Uqcr11	7
Atp5a1	9	Cdc42	8	Atp5c1	7
Cox4i1	9	Hspa1b	8	Calm1	7
Cycs	9	Nfkbia	8	Fos	7
Gapdh	9	Pcna	8	Hspe1	7
Hsp90aa1	9	Ppp2ca	8	Rpl29	7
Rplp0	9	Rac2	8	Rpl5	7
Rps6	9	Rhoa	8		
Actg1	8	Rps3a	8		

3 DISCUSSION

As AKI could result in high mortality, it is important to take back to homeostasis by a suitable way[4]. The $CD11b^{+}/Ly6C^{int}$ population is identified as wound healing population, which carries membrane receptors and chemokines associated with inflammation at the same time[14]. Understanding how the population changes may provide a new way to treat AKI by modulating the immune system.

In our study, we identified nine gene profiles, most of which were downregulated after IRI. The proportion of $CD11b^{+}/Ly6C^{int}$ macrophages was at a maximum one day after IRI and was markedly reduced at day 9 after IRI. Taking this into consideration, the genes in the profile 13 were involved in infiltration and proliferation. GO analysis of profile 13 showed that the genes related to the extracellular vesicular exosome were significantly changed, which was consistent with the finding that $CD11b^{+}/Ly6C^{int}$ macrophage could secrete anti-inflammation cytokines[15]. GO and pathway analysis indicated that immune cell chemotaxis (for example, neutrophil, leukocyte, lymphocyte, monocyte, and macrophage) and G1/S progression were downregulated at later time points. In mitochondria, the oxidation-reduction process and respiratory electron transport were significantly involved after IRI as Atp5a1, Atp5o, and Cox4i1 are also key genes in the PPI network. It would be required to further assess the vitality, switch and infiltration ability of $CD11b^{+}/Ly6C^{int}$ macrophages, given that Cdc42 and Rac2 were found to have an effect on apoptosis, migration, and M1-M2 differentiation[24, 25].

Protein phosphatase 2A (Pp2a) is a bona fide tumor suppressor gene that is involved in mitosis and apoptosis[26]. Homologues Ppp2ca (Pp2ac) and Ppp2cb are the catalytic subunits of Pp2a[27]. Previous studies have shown that upregulation of Ppp2ca in systemic lupus erythematosus decreased IL-2[28], resulting in the generation of effector and memory T cells and the maintenance of regulatory T cells[29]. Moreover, it was suggested that reduction of Ppp2ca may play a role in anti-inflammatory progression by increasing osteoprotegerin (OPG) expression and decreasing receptor activator of nuclear factor κB ligand (RANKL) expression[30]. In prostate cancer cells, loss of Ppp2ca facilitated epithelial-to-mesenchymal transition[31]. Taken together, the reduction of Ppp2ca in profile 13 may be a reason why $CD11b^{+}/Ly6C^{int}$ macrophages decreased inflammation.

Rpl5 can induce the cell cycle, and the downregulation of Rpl5 at day 9 after IRI may provide an explanation of the reduction of $CD11b^{+}/Ly6C^{int}$ macrophages. Moreover, the depletion of Rpl5 strongly suppresses cell cycle progression in primary human lung fibroblasts[32]. Rpl5 and Rpl11 promote apoptosis and reduce cellular proliferation in tumor *in vitro*[33]. However, it has also been reported that a heterozygous deletion or mutated Rpl5 occurred in 11% of glioblastoma, 28% of melanoma and 34% of breast cancer cases[34].

Nhp2, one of the key nodes in PPI, was significantly decreased when 1-day and 9-day $CD11b^{+}/Ly6C^{int}$ macrophages were compared. Nhp2 is a part of H/ACA ribonucleoprotein particles (RNPs), containing four common proteins, including the pseudouridine synthase Cbf5, Nhp2, Nop10, Gar1a and a substrate-specific H/ACA RNA. H/ACA is considered to play a role in the biogenesis of spliceosomal small nuclear RNA (snRNA) and ribosomal RNA (rRNA)[35]. Depletion of Nhp2 reduced all H/ACA snoRNAs and impaired global rRNA pseudouridylation, which play a role in the uridine selection or isomerization processes as they are required for the synthesis and stability of particles[36, 37].

Nhp2 is highly expressed in spleen, thymus, small intestine, testis, ovary, prostate, colon (mucosal lining), skeletal muscle, kidney, heart, pancreas, placenta, and brain, whereas the expression levels in the liver are low[38]. Nhp2 mRNA was barely detectable in peripheral blood leukocytes and lung. During the differentiation of U937 cells into monocytes and macrophages induced by 12-O-tetradecanoylphorbol-13-acetate (TPA), the expression of Nhp2 mRNA was markedly decreased, but was upregulated during the retro-differentiation[38]. Nhp2, hTR, hTERT and Nop10 could control telomere homeostasis, which is important for

apoptosis and cell-cycle arrest[39, 40]. Thus, Nhp2 may affect the polarization of macrophage.

Finally, it is important to identify which genes could serve as reference genes. We analysed the expression levels of Gapdh, Actb, B2m, Hmbs, Hprt, Rplp0, Tbp, Gusb, Ppia, Oaz1, Nono, Tfrc, Eef2, Hsb90ab1, Rps18, Sdha, Ywhaz, Ubc, Rps17, Rplp0, Rpl37a, Pum1, Psmc4, Pop4, Pgk1, Pes1, Mrpl9, Ipo80, Gadd45a, Elf1, Eif2b1, Cdkn1b, Cdkn1a, Casc3, Abl1, and Pol2a which are widely used[41–43]. The data showed that RPS18 may be an appropriate reference gene as its expression was stable in macrophages after renal IRI.

In our study, a total of 6738 DEGs were found. We analysed the genes that were stable at early time, but were abruptly downregulated at late time, investigated the function and molecular pathways that they were involved, and studied the critical genes involved. A possible explanation why $CD11b^{+}/Ly6C^{int}$ macrophages were reduced on day 9 may be due to the fact that genes involved in the chemotaxis and proliferation were decreased. On the other hand, one of the key genes, Nhp2, may be involved in the polarization of macrophages. Taken together, our study will increase insight into the functional changes of macrophages; therefore, identifying the critical genes involved may provide novel targets for regulating the quantity and phenotype of macrophages.

Conflict of Interest Statement

The authors report no conflicts of interest. The authors alone are responsible for the content and writing of the paper.

REFERENCES

1 Hsu CN, Lee CT, Su CH, *et al*. Incidence, outcomes, and risk factors of community-acquired and hospital-acquired acute kidney injury: A Retrospective Cohort Study. Medicine (Baltimore), 2016,95(19):e3674

2 Xu G, Player P, Shepherd D, *et al*. Identifying acute kidney injury in the community--a novel informatics approach. J Nephrol, 2016,29(1):93-98

3 Ranganathan PV, Jayakumar C, Mohamed R, *et al*. Netrin-1 regulates the inflammatory response of neutrophils and macrophages, and suppresses ischemic acute kidney injury by inhibiting COX-2-mediated PGE2 production. Kidney Int, 2013,83(6):1087-1098

4 Ponce D, Dias DB, Nascimento GR, *et al*. Long-term outcome of severe acute kidney injury survivors followed by nephrologists in a developing country. Nephrology (Carlton), 2016,21(4):327-334

5 Mehta RL, Burdmann, EA, Cerda J, et al. Recognition and management of acute kidney injury in the International Society of Nephrology 0by25 Global Snapshot: a multinational cross-sectional study. Lancet, 2016,387(10032):2017-2025

6 Hou L, Chen G, Feng B, et al. Small interfering RNA targeting TNF-alpha gene significantly attenuates renal ischemia-reperfusion injury in mice. J Huazhong Univ Sci Technolog Med Sci, 2016,36(5):634-638

7 Martina MN, Noel S, Saxena A, *et al*. Double-negative alphabeta T cells are early responders to AKI and are found in human kidney. J Am Soc Nephrol, 2016,27(4):1113-1123

8 Karasawa K, Asano K, Moriyama S, *et al*. Vascular-resident CD169-positive monocytes and macrophages control neutrophil accumulation in the kidney with ischemia-reperfusion injury. J Am Soc Nephrol, 2015,26(4):896-906

9 Liang S, Wang W, Gou X. MicroRNA 26a modulates regulatory T cells expansion and attenuates renal ischemia-reperfusion injury. Mol Immunol, 2015,65(2):321-327

10 Huen SC, Huynh L, Marlier A, *et al*. GM-CSF promotes macrophage alternative activation after renal ischemia/reperfusion injury. J Am Soc Nephrol, 2015,26(6):1334-1345

11 Lee S, Huen S, Nishio H, *et al*. Distinct macrophage phenotypes contribute to kidney injury and repair. J Am Soc Nephrol, 2011,22(2):317-326

12 Huen SC, Cantley LG. Macrophage-mediated injury and repair after ischemic kidney injury. Pediatr Nephrol, 2015,30(2):199-209

13 Cao Q, Wang Y, Wang XM, *et al*. Renal F4/80+ CD11c+ mononuclear phagocytes display phenotypic and functional characteristics of macrophages in health and in adriamycin nephropathy. J Am Soc Nephrol, 2015,26(2):349-363

14 Clements M, Gershenovich M, Chaber C, *et al*. Differential Ly6C expression after renal ischemia-reperfusion identifies unique macrophage populations. J Am Soc Nephrol, 2016,27(1):159-170

15 Dragomir AC, Sun R, Choi H, *et al*. Role of galectin-3 in classical and alternative macrophage activation in the liver following acetaminophen intoxication. J Immunol, 2012,189(12):5934-5941

16 Rudnick PA, Wang X, Yan X, *et al*. Improved normalization of systematic biases affecting ion current measurements in label-free proteomics data. Mol Cell Proteomics, 2014,13(5):1341-1351

17 Zhao YH, Zhang XF, Zhao YQ, *et al*. Time-series analysis in imatinib-resistant chronic myeloid leukemia K562-cells under different drug treatments. J Huazhong Univ Sci Technolog Med Sci, 2017,37(4):621-627

18 Gao A, Yang J, Yang G, *et al*. Differential gene expression profiling analysis in workers occupationally exposed to benzene. Sci Total Environ, 2014,472(872-879)

19 Pathan M, Keerthikumar S, Ang CS, *et al*. FunRich: An open access standalone functional enrichment and interaction network analysis tool. Proteomics, 2015,15(15):2597-2601

20 Wang ZX, Zhou CX, Elsheikha HM, *et al*. Proteomic Differences between Developmental Stages of Toxoplasma gondii Revealed by iTRAQ-Based Quantita-

tive Proteomics. Front Microbiol, 2017,8(985):1-15
21 Cong F, Liu X, Han Z, *et al*. Transcriptome analysis of chicken kidney tissues following coronavirus avian infectious bronchitis virus infection. BMC genomics, 2013,14(743):1-13
22 Chin CH, Chen SH, Wu HH, *et al*. cytoHubba: identifying hub objects and sub-networks from complex interactome. BMC Syst Biol, 2014,8 Suppl 4(S11):1-7
23 Chen H, Chai W, Li B, *et al*. Effects of beta-catenin on differentially expressed genes in multiple myeloma. J Huazhong Univ Sci Technolog Med Sci, 2015,35(4):546-552
24 DiCosmo-Ponticello CJ, Hoover D, Coffman FD, *et al*. MIF inhibits monocytic movement through a non-canonical receptor and disruption of temporal Rho GTPase activities in U-937 cells. Cytokine, 2014,69(1):47-55
25 Joshi S, Singh AR, Zulcic M, *et al*. Rac2 controls tumor growth, metastasis and M1-M2 macrophage differentiation in vivo. PLoS One, 2014,9(4):e95893
26 Sablina AA, Hahn WC. SV40 small T antigen and PP2A phosphatase in cell transformation. Cancer Metastasis Rev, 2008,27(2):137-146
27 Pan X, Chen X, Tong, X, *et al*. Ppp2ca knockout in mice spermatogenesis. Reproduction, 2015,149(4):385-391
28 Katsiari CG, Kyttaris VC, Juang YT, *et al*. Protein phosphatase 2A is a negative regulator of IL-2 production in patients with systemic lupus erythematosus. J Clin Invest, 2005,115(11):3193-3204
29 Barron L, Dooms H, Hoyer KK, *et al*. Cutting edge: mechanisms of IL-2-dependent maintenance of functional regulatory T cells. J Immunol, 2010,185(11):6426-6430
30 Okamura H, Yang D, Yoshida K, *et al*. Protein phosphatase 2A Calpha is involved in osteoclastogenesis by regulating RANKL and OPG expression in osteoblasts. FEBS Lett, 2013,587(1):48-53
31 Bhardwaj A, Singh S, Srivastava SK, *et al*. Restoration of PPP2CA expression reverses epithelial-to-mesenchymal transition and suppresses prostate tumour growth and metastasis in an orthotopic mouse model. Br J Cancer, 2014,110(8):2000-2010
32 Teng T, Mercer CA, Hexley P, *et al*. Loss of tumor suppressor RPL5/RPL11 does not induce cell cycle arrest but impedes proliferation due to reduced ribosome content and translation capacity. Mol Cell Biol, 2013,33(23):4660-4671
33 Zhou X, Hao Q, Zhang Q, *et al*. Ribosomal proteins L11 and L5 activate TAp73 by overcoming MDM2 inhibition. Cell Death Differ, 2015,22(5):755-766
34 Fancello L, Kampen KR, Hofman IJ, *et al*. The ribosomal protein gene RPL5 is a haploinsufficient tumor suppressor in multiple cancer types. Oncotarget, 2017,8(9):14462-14478
35 Wu H, Feigon J. H/ACA small nucleolar RNA pseudouridylation pockets bind substrate RNA to form three-way junctions that position the target U for modification. Proc Natl Acad Sci U S A, 2007,104(16):6655-6660
36 Watkins NJ, Gottschalk A, Neubauer G, *et al*. Cbf5p, a potential pseudouridine synthase, and Nhp2p, a putative RNA-binding protein, are present together with Gar1p in all H BOX/ACA-motif snoRNPs and constitute a common bipartite structure. RNA, 1998,4(12):1549-1568
37 Henras A, Henry Y, Bousquet-Antonelli C, *et al*. Nhp2p and Nop10p are essential for the function of H/ACA snoRNPs. EMBO J, 1998,17(23):7078-7090
38 Kang HS, Jung HM, Jun DY, *et al*. Expression of the human homologue of the small nucleolar RNA-binding protein NHP2 gene during monocytic differentiation of U937 cells. Biochim Biophys Acta, 2002,1575(1-3):31-39
39 Li S, Duan J, Li D, *et al*. Structure of the Shq1-Cbf5-Nop10-Gar1 complex and implications for H/ACA RNP biogenesis and dyskeratosis congenita. EMBO J, 2011,30(24):5010-5020
40 Colgin LM, Reddel RR. Telomere maintenance mechanisms and cellular immortalization. Curr Opin Genet Dev, 1999,9(1):97-103
41 Li B, Matter EK, Hoppert HT, *et al*. Identification of optimal reference genes for RT-qPCR in the rat hypothalamus and intestine for the study of obesity. Int J Obes (Lond), 2014,38(2):192-197
42 Eissa N, Kermarrec L, Hussein H, *et al*. Appropriateness of reference genes for normalizing messenger RNA in mouse 2,4-dinitrobenzene sulfonic acid (DNBS)-induced colitis using quantitative real time PCR. Sci Rep, 2017,7(42427):1-13
43 Tan SC, Ismail MP, Duski DR, *et al*. Identification of optimal reference genes for normalization of RT-qPCR data in cancerous and non-cancerous tissues of human uterine cervix. Cancer Invest, 2017,35(3):163-173

(Received Aug. 20, 2017; revised Nov. 8, 2017)